

Article

Organic Solvent Free Process to Fabricate High Performance Silicon/Graphite Composite Anode

Chen Fang ^{1,†}, Haiqing Xiao ^{1,2,†}, Tianyue Zheng ^{1,3,*}, Hua Bai ^{2,*} and Gao Liu ^{1,*}

¹ Energy Storage and Distributed Resources Division, Lawrence Berkeley National Laboratory, Berkeley, CA 94720, USA; cfang@lbl.gov (C.F.); xiaohaiqing@hotmail.com (H.X.)

² Institute of Industrial and Consumer Products Safety, Chinese Academy of Inspection and Quarantine (CAIQ), Beijing 100176, China

³ Ningbo Institute of Materials Technology and Engineering, Chinese Academy of Sciences, Ningbo 315201, China

* Correspondence: tyzheng@nimte.ac.cn (T.Z.); bai111@sina.com (H.B.); gliu@lbl.gov (G.L.)

† These authors contributed equally to this work.

Abstract: Cycling stability is a key challenge for application of silicon (Si)-based composite anodes as the severe volume fluctuation of Si readily leads to fast capacity fading. The binder is a crucial component of the composite electrodes. Although only occupying a small amount of the total composite mass, the binder has major impact on the long-term electrochemical performance of Si-based anodes. In recent years, water-based binders including styrene-butadiene rubber (SBR) and carboxymethyl cellulose (CMC) have attracted wide research interest as eco-friendly and low-cost alternatives for the conventional poly(vinylidene difluoride) (PVDF) binder in Si anodes. In this study, Si-based composite anodes are fabricated by simple solid mixing of the active materials with subsequent addition of SBR and CMC binders. This approach bypasses the use of toxic and expansive organic solvents. The factors of binder, silicon, and graphite materials have been systematically investigated. It is found that the retained capacities of the anodes are more than 440 mAh/g after 400 cycles. These results indicate that organic solvent free process is a facile strategy for producing high performance silicon/graphite composite anodes.

Keywords: lithium-ion batteries; water-based binders; styrene-butadiene rubber (SBR); carboxymethyl cellulose (CMC); silicon; graphite; anode



Citation: Fang, C.; Xiao, H.; Zheng, T.; Bai, H.; Liu, G. Organic Solvent Free Process to Fabricate High Performance Silicon/Graphite Composite Anode. *J. Compos. Sci.* **2021**, *5*, 188. <https://doi.org/10.3390/jcs5070188>

Academic Editor:
Francesco Tornabene

Received: 9 June 2021
Accepted: 14 July 2021
Published: 17 July 2021

Publisher's Note: MDPI stays neutral with regard to jurisdictional claims in published maps and institutional affiliations.



Copyright: © 2021 by the authors. Licensee MDPI, Basel, Switzerland. This article is an open access article distributed under the terms and conditions of the Creative Commons Attribution (CC BY) license (<https://creativecommons.org/licenses/by/4.0/>).

1. Introduction

Advanced rechargeable batteries are currently being developed to power a variety of appliances, ranging from portable devices like smartphones to large-scale equipment including electric vehicles and grid energy-storage systems [1–5]. A large number of studies have focused on the development of high-capacity composite electrodes to enhance the energy density and performance of the next-generation rechargeable batteries [6,7]. In particular, silicon (Si) is theoretically expected to provide about ten times higher capacity (ca. 3579 mAh/g) for lithium-ion batteries (LIBs) than that of the commercialized graphite anode (ca. 370 mAh/g) [8–10]. However, the practical applications of Si materials have been hindered by their severe volume changes during the repetitive lithiation and delithiation cycles which could readily lead to loss of electrical contact and thus fast capacity fading and even battery failure [11,12]. In order to solve the volume change problem, researchers have developed nanostructured Si anode materials as well as composite Si materials [13,14]. Nanostructured Si materials face considerable challenges in large-scale application due to their complicated preparation technologies. On the other hand, composite electrodes are promising in industrial application due to their mature and flexible fabrication processes. Generally, binders only occupy a small mass percentage of the composite electrodes, and therefore, the engineering of these polymer components is a cost-efficient approach to

improve the performance of the active materials, including Si anodes materials [15–18]. In particular, the binders in Si electrodes play a crucial role as binders can accommodate the dramatic volume change of silicon active materials [19].

Conventionally, poly (vinylidene difluoride) (PVDF) binder is widely used for Li-ion cells due to its good electrochemical stability and binding capability. However, the process using PVDF normally requires the use of organic solvents like N-methyl-2-pyrrolidone (NMP), which is potentially hazardous and high-cost [15,20]. Therefore, it is beneficial to develop binders that can be processed with non-toxic solvents. Recently, it was reported that water-based binders such as styrene-butadiene rubber (SBR) and carboxymethyl cellulose (CMC) can effectively improve the cycling stability of silicon composite electrodes [21–23]. According to Hochgatterer et al. [24], the formation of covalent bonding between CMC and silicon particle plays an important role in the effective binding and thus improved cell performance. Buqa et al. [21] and Liu et al. [25] found that the capacity retention of Si was significantly improved by using SBR and CMC binders. The authors noted that the addition of SBR helps to enhance the elasticity of the laminate since CMC is extremely brittle. Li et al. [26], however, showed that the Si with only CMC binder has better performance than both the SBR/CMC binder and the PVDF binder. Because the SBR mixture binder shows greater adhesion strength and larger breakage elongation, it can better adhere to the particles and current collector to withstand a greater level of stress during volume expansion with reversibility. Dimov et al. [27] reported that SBR and CMC are the most crucial components for the improved cycle life of silicon/carbon (Si/C) electrodes. The CMC/SBR binder has a favorable impact on the cycle life of Si electrodes presumably due to the increased strength of the electrode film. These reports demonstrate that CMC/SBR is a promising binder system for application of silicon anodes in LIBs although it is necessary to examine the impact of CMC/SBR binder ratio.

In this study, Si and graphite are used as the active materials in composite anodes for LIBs, which are fabricated via solid mixing with subsequently addition of water-based SBR and CMC binders to produce high-performance anodes. The utilization of simple solid mixing and aqueous fabrication conditions is aimed at practical application of the materials in large-scale production. It is particularly helpful to employ water as solvent to avoid the toxic and high-cost organic solvents (e.g., NMP) in electrode fabrication. The impact of CMC and SBR binder ratio was systematically examined in full range, and the performance of a few commercially available SBR binders are investigated. In addition, other composite factors including silicon particle size and choice of graphite are also studied. The anodes with CMC/SBR binder have demonstrated promising cycling performance. This study demonstrates an effective composite electrode fabrication method for practical application of silicon-based anodes in LIBs.

2. Materials and Methods

2.1. Materials

Styrene-butadiene rubber (SBR) emulsions (JSR Corporation, Japan), JSR1: JSR SX8684(A)-64 (41.3 wt.%), JSR2: JSR S2910(J)-17 (26.4 wt.%), JSR3: JSR TRD105A (40.7 wt.%). Carboxymethyl cellulose, sodium salt (CMC) (Aldrich), Mw 250,000, D. S. 0.90. The 4 wt.% CMC solution was made by dissolving 4 g CMC in 96 g deionized water. Conductive Carbon Black: TIMCAL SUPER C45. Si nanoparticles, 50–70 nm (Sigma-Aldrich). Si micro-particles were obtained from Argonne National Laboratory (ANL). Graphite: Hitachi magE. Composite Graphite (ConocoPhillips): CGP-G8.

2.2. Composite Electrode Preparation

Graphite, silicon particles and conductive black were firstly mixed and milled in an agate mortar for 15 min. Then the CMC solution was added with further milling over 15 min. Lastly, SBR emulsion and deionized water were added and the mixture was milled for another 15 min. The obtained slurry was casted on copper foil by a 150 μm blade. The electrode films were dried at room temperature for 3 h followed by heating under vacuum

condition at 60 °C for 24 h. The electrodes were compressed to around 40 µm thick using a rolling mill. The loading of the composite materials on the electrode was 4 mg/cm². It should be noted here that the dry mixing method was chosen in this study to develop a protocol readily adoptable in industry at low cost. In addition, solid mixing is needed to ensure homogeneous distribution of silicon and graphite materials in the final electrode composites. Due to the homogeneous spread of silicon and graphite materials, there would not be loss of silicon materials during slurry preparation and casting in aqueous solution.

2.3. Coin Cell Fabrication and Testing

2325 coin cells were used to fabricate the half cells of the composite electrodes against lithium film counter electrodes with Celgard separator under argon atmosphere. 1.2 M LiPF₆ ethylene carbonate:diethyl carbonate (EC:DEC, 3:7 *w/w*) electrolyte was used with 30 wt.% fluoroethylene carbonate (FEC) as electrolyte. The electrochemical performance of the cells was evaluated in a thermal chamber at 30 °C with a Maccor Battery Test System. Cycling procedure includes two formation cycles of C/25, followed by C/10 or C/3 cycles. The electrochemical testing window was 0.005 to 1.0 V vs. Li/Li⁺.

2.4. Characterization

The peeling test was performed with a piece of the prepared electrode on copper foil on a tensile instrument (TCD225 Series Digital Force Tester). The electrode piece was attached to the peel stage with double side tape from the back side, and the surface of the electrode was covered with 3M tape to perform peeling. For the peeling test, the 3M tape was dragged at the 180-degree direction. The scanning electron microscopy (SEM) characterization of composite electrodes were carried out with JSM-7500F (JOEL Ltd.) under high vacuum at room temperature, and the Energy-dispersive X-ray spectroscopy (EDX) data was collected with an EDX spectrometer incorporated with the SEM.

3. Results

3.1. The Effect of CMC and SBR Ratio

Figure 1 shows the cycling performance of composite anodes made with different ratio of CMC and SBR binders under C/10 (1C = 1000 mA/g). JSR1 is used as the SBR component here and the impact of different types of SBR binders (JSR1, JSR2, JSR3) will be investigated in later section. The formulation of the anodes was CGP-G8 (Graphite)/Si (micro-size)/C45/binder = 73/15/2/10 (wt.%). The total mass of binder accounted for 10% of the electrode mass, and the ratio of CMC and JSR1 varied from 1/9 to 10/0 (*w/w*). The composite electrode with 0/10 CMC/JSR1 binder (namely SBR-only binder) failed to deliver sufficient mechanical robustness for testing and thus was not included in the figure. This section aims to systematically examine the influence of the ratio of CMC:SBR binders on composite electrode performance.

The results indicate that incorporation of CMC in the binder helped to improve the cycling performance of the electrodes, but over-high CMC ratio could however negatively impact the cell performance. The electrode made with CMC/JSR1 = 4/6 shows the best performance. This is likely because that balanced property of the Si composite was achieved with this ratio, where CMC provides adhesion force while JSR1 realizes elasticity that could accommodate Si volume change to improve the reversible capacity of Si anode [21,25]. The peel test (Figure 2) shows that all the electrodes have strong adhesion force, indicating that the combination of CMC and SBR can adhesively bind the Si and graphite materials together to maintain electrode integrity, which is crucial for improving the cycling stability.

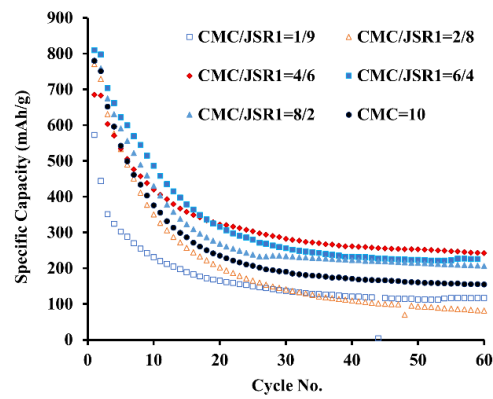


Figure 1. Cycling performance of anodes made of different binder ratios of CMC and SBR (JSR1) under C/10. Electrode composition: CGP-G8/Si/C45/binder = 73/15/2/10 (wt.%).

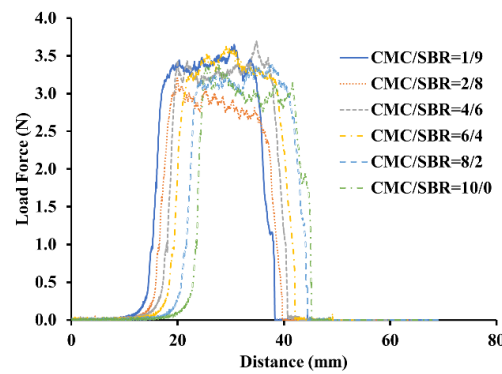


Figure 2. Peel test results of anodes made of different binder ratios of CMC and SBR.

3.2. The Effect of Silicon Particle Size

The size of silicon particle plays an important role in the cycling stability of Si-based anodes [28–31]. Cells fabricated with micro-sized and nano-sized Si materials are studied here to investigate the size effect of Si particles. To simplify the electrode design, only CMC is used as the binder. The cycle performance testing is under C/10 (1C = 1000 mA/g). As shown in Figure 3, the micro-sized Si electrode delivered a specific capacity of almost 800 mAh/g in the initial cycle with however a faster capacity decay and much lower capacity after 80 cycles (about 150 mAh/g). In comparison, the nano-sized Si showed a comparable initial capacity at about 750 mAh/g and delivered stable reversible capacity of about 500 mAh/g after 80 cycles. The higher capacity retention of nano-sized Si likely benefited from its higher intercalation/deintercalation rates and the buffering effect for volume change with nano-sized particles [15].

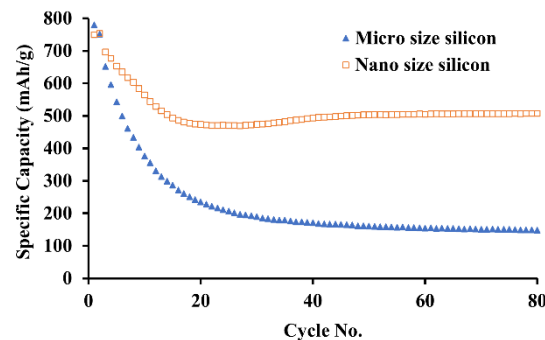


Figure 3. Cycling performance of micro-size and nano-size Si composite anode. Electrode composition: CGP-G8/Si/C45/binder = 73/15/2/10 (wt.%).

3.3. The Selection of Graphite Materials

Two types of graphite (CGP-G8 and magE) were used to investigate the impact of graphite materials on the cycle performance of anode. CGP-G8 is a type of composite graphite which was chosen as baseline graphite for BATT program [32] and magE is artificial graphite with a high volume of internal pores. The cycling performance of the nano-sized silicon anodes with different graphite materials under C/10 ($1C = 1000 \text{ mA/g}$) is illustrated in Figure 4. It can be observed that the first cycle specific capacities of the anodes made from CGP-G8 and magE were comparably at 749.8 and 813.7 mAh/g, respectively. Both types of electrodes experienced an initial decay of performance in the first 20 cycles and then recovered. The stabilized capacity for the electrode using CGP-G8 graphite was around 500 mAh/g while that for the magE was around 700 mAh/g. This indicates that the internal pores of magE are likely a positive factor for good cycle performance of Si anode. Silicon/MagE composite after solid mixing has been characterized by SEM. It was found that the silicon nanoparticles were evenly distributed across the graphite surface (Figure S1a in Supplementary Materials). Energy-dispersive X-ray spectroscopy (EDX) analysis (Figure S1b,c) of the composite also demonstrates that the silicon element was uniformly present on the graphite surface. These results confirmed the effectiveness of the solid mixing protocols employed in electrode slurry preparation.

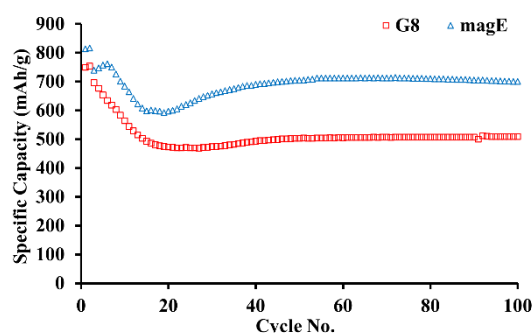


Figure 4. Cycling performance of Si composite anode prepared with CGP-G8 and magE graphite materials.

3.4. The Selection of SBR Binders

Buqa et al. [21] reported that as low as 1–2% of SBR mixed with 1–2% Na-CMC as binder was sufficient to assure a good electrochemical performance of nano-silicon/graphite electrodes. It is consistent with the results shown in Figure 1, which indicates that the optimized ratio of CMC and SBR is around 4/6. Adopting this ratio and using magE graphite and nano-sized Si as the active materials (as determined in earlier sections), the performance of different types of SBR emulsions was tested. Three types of SBR emulsions, JSR1, JSR2 and JSR3, are studied and the results are shown in Figure 5. The peel test results are showed in Figure 6. The three electrodes showed similar cycling trend with first cycle specific capacities between 610 and 680 mAh/g and the first cycle coulombic efficiency higher than 88%, which is comparable to those of graphite anodes [32]. After initial decay in the first 20 cycles, the three electrodes were able to maintain stable performances over 400 cycles, where 72–75% of the initial capacities were retained. JSR1 and JSR3 delivered high retained specific capacities of close to 500 mAh/g and also high coulombic efficiency (CE) above 99.5%. It is worth noting here that the CEs of the cells could be maintained around 99.8–99.9% level after 400 cycles, which is critical for practical application in batteries (full cells) where lithium inventory is limited. The electrode with JSR2 shows slightly lower capacity (442 mAh/g) than that of JSR1 and JSR3, which could be rationalized by its lowest adhesion force among the three electrodes (Figure 6). A detailed examination of the cycling performance is performed with differential capacity (dQ/dV) curves and charge/discharge curves in Figure S2 and the corresponding discussion in the Supplementary Materials. The charge/discharge curves provided extra evidence of stable

cycling performance of the electrodes while the differential capacity curves indicated the degradation of silicon materials during cycling that presumably led to capacity decay of the electrodes.

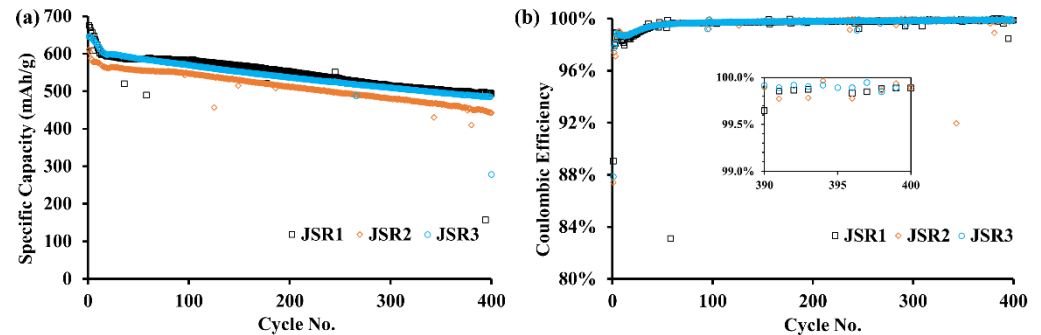


Figure 5. The cycling performance of Si/C composite anodes using different SBR binders under C/3 (1C = 750 mA/g) with constant voltage during each discharge step (a) specific capacity and (b) Coulombic efficiency (insert shows the last 10 cycles).

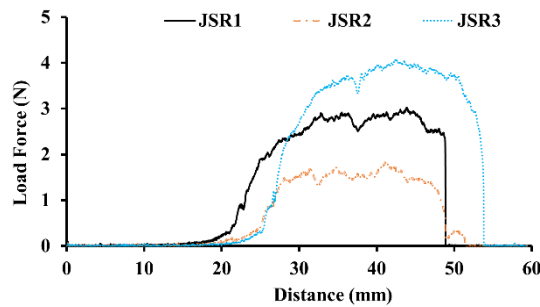


Figure 6. Peer test results of anodes made of different SBR binder (JSR1, JSR2 and JSR3).

3.5. Morphology Changes of the Si/C Composite Electrode after Cycling

To illustrate the mechanism for performance change of Si/graphite composite anode during cycling, the morphologies of electrodes before and after cycling have been analyzed. As shown in Figure 7a,b, the electrode surface before cycling was smooth and tidy, where the active particles were firmly integrated. It needs to be noted here that there were void spaces on the fresh composite electrode, which resembles cracks formed after cell cycling. These features were formed with the solid mixing under aqueous conditions. There were no long-range cracks or highly interconnected channels observed on the fresh electrodes. As shown in Figure 7c, there were many conductive particles distributed on the surface of active particles, and the surface of the active particles was smooth with clear boundaries before cycling. However, after cycling, many cracks were observed on the electrode surface (Figure 7d), and there were gaps between active particles (Figure 7e). The cracks were present across long distances, and they formed interconnected channels. These features resulted from the dramatic volume change of silicon component during cycling. Conductive particles could no longer be clearly observed on the active particles, the surfaces of which were rough without clear boundaries (Figure 7f). These changes led to lower conductivity of the composite, which in turn caused the capacity fading of the electrode.

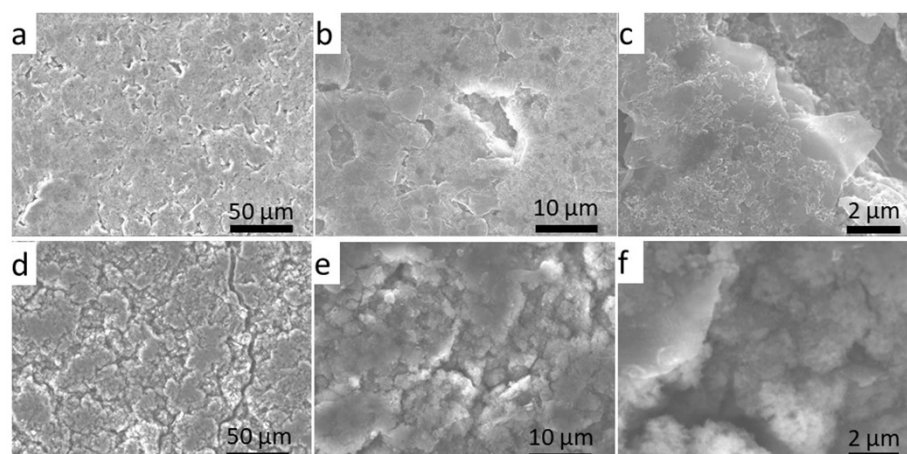


Figure 7. Morphology images of the Si/C composite electrodes. The formulation of the anodes was magE/nanoSi/C45/CMC/JSR3 = 82.9/9.2/2.5/3/2.4 (wt.%). (a–c) The SEM images of the anode before cycling. (d–f) The SEM images of the anode after cycling.

4. Conclusions

In this work, we studied the effects of binders on the cycling performance of the Si-based composite anodes. The results indicate that combined CMC/SBR binder materials can achieve better cycling performance than single-component CMC binder. The optimum ratio of CMC and SBR was found to be 4/6 (*w/w*). It is also found that decreasing the size of Si from micro-size to nano-size and substituting CGP-G8 graphite with magE can significantly improve the cycle performance of the Si/C composite anodes. Lastly, high performance anodes were made with magE (graphite), nano-Si, C45 (conductive additive) and CMC/SBR binder. The electrode fabrication process utilized simple solid mixing of the active materials and aqueous mixing of the active materials with binders, which is environmentally friendly and can be readily adopted in large-scale application.

Supplementary Materials: The following are available online at <https://www.mdpi.com/article/10.3390/jcs5070188/s1>, Figure S1: Characterization of silicon/graphite composite after solid mixing (a) SEM image and (b,c) EDX mapping, Figure S2: Differential capacity (dQ/dV) curves and charge/discharge curves of electrodes prepared with JSR1, JSR2 JSR3.

Author Contributions: Conceptualization, H.X., H.B., T.Z. and G.L.; methodology, H.X. and T.Z.; validation, H.X. and T.Z.; investigation, H.X. and T.Z.; writing—original draft preparation, H.X.; writing—review and editing, C.F., T.Z. and G.L.; visualization, C.F. and H.X.; supervision, T.Z., H.B. and G.L.; project administration, G.L. All authors have read and agreed to the published version of the manuscript.

Funding: This research was funded by the Assistant Secretary for Energy Efficiency, Vehicle Technologies Office of the U.S. Department of Energy, under the Silicon Consortium Program.

Acknowledgments: Electron microscopy experiments were conducted at the Molecular Foundry, which is located at Lawrence Berkeley National Laboratory. Work at the Molecular Foundry was supported by the Office of Science, Office of Basic Energy Sciences, of the U.S. Department of Energy under Contract No. DE-AC02-05CH11231. H.X. acknowledges support from National key R & D program of China (2017YFF0210703).

Conflicts of Interest: The authors declare no conflict of interest.

References

1. Armand, M.; Tarascon, J.M. Building better batteries. *Nature* **2008**, *451*, 652–657. [[CrossRef](#)]
2. Fang, C.; Zhang, G.; Lau, J.; Liu, G. Recent advances in polysulfide mediation of lithium-sulfur batteries via facile cathode and electrolyte modification. *APL Mater.* **2019**, *7*, 080902. [[CrossRef](#)]

3. Zhao, Y.; Fang, C.; Zhang, G.; Hubble, D.; Nallapaneni, A.; Zhu, C.; Zhao, Z.; Liu, Z.; Lau, J.; Fu, Y.; et al. A Micelle Electrolyte Enabled by Fluorinated Ether Additives for Polysulfide Suppression and Li Metal Stabilization in Li-S Battery. *Front. Chem.* **2020**, *8*, 484. [[CrossRef](#)]
4. Hopkins, E.J.; Frisco, S.; Pekarek, R.T.; Stetson, C.; Huey, Z.; Harvey, S.; Li, X.; Key, B.; Fang, C.; Liu, G.; et al. Examining CO₂ as an Additive for Solid Electrolyte Interphase Formation on Silicon Anodes. *J. Electrochem. Soc.* **2021**, *168*, 030534. [[CrossRef](#)]
5. Fang, C.; Lau, J.; Hubble, D.; Khomein, P.; Dailing, E.A.; Liu, Y.; Liu, G. Large-Molecule Decomposition Products of Electrolytes and Additives Revealed by On-Electrode Chromatography and MALDI. *Joule* **2021**, *5*, 415–428. [[CrossRef](#)]
6. Chen, H.; Yang, Y.; Boyle, D.T.; Jeong, Y.K.; Xu, R.; de Vasconcelos, L.S.; Huang, Z.; Wang, H.; Wang, H.; Huang, W.; et al. Free-standing ultrathin lithium metal–graphene oxide host foils with controllable thickness for lithium batteries. *Nat. Energy* **2021**, 1–9. [[CrossRef](#)]
7. Zhou, S.; Fang, C.; Song, X.; Liu, G. Highly Ordered Carbon Coating Prepared with Polyvinylidene Chloride Precursor for High-Performance Silicon Anodes in Lithium-Ion Batteries. *Batter. Supercaps* **2021**, *4*, 240–247. [[CrossRef](#)]
8. Wang, H.; Fu, J.; Wang, C.; Wang, J.; Yang, A.; Li, C.; Sun, Q.; Cui, Y.; Li, H. A binder-free high silicon content flexible anode for Li-ion batteries. *Energy Environ. Sci.* **2020**, *13*, 848–858. [[CrossRef](#)]
9. Asenbauer, J.; Eisenmann, T.; Kuenzel, M.; Kazzazi, A.; Chen, Z.; Bresser, D. The success story of graphite as a lithium-ion anode material—Fundamentals, remaining challenges, and recent developments including silicon (oxide) composites. *Sustain. Energy Fuels* **2020**, *4*, 5387–5416. [[CrossRef](#)]
10. Fang, C.; Liu, Z.; Lau, J.; Elzouka, M.; Zhang, G.; Khomein, P.; Lubner, S.; Ross, P.N.; Liu, G. Gradient Polarity Solvent Wash for Separation and Analysis of Electrolyte Decomposition Products on Electrode Surfaces. *J. Electrochem. Soc.* **2020**, *167*, 020506. [[CrossRef](#)]
11. Zhou, Y.; Yang, Y.; Hou, G.; Yi, D.; Zhou, B.; Chen, S.; Lam, T.D.; Yuan, F.; Golberg, D.; Wang, X. Stress-relieving defects enable ultra-stable silicon anode for Li-ion storage. *Nano Energy* **2020**, *70*, 104568. [[CrossRef](#)]
12. Zhou, S.; Fang, C.; Song, X.; Liu, G. The influence of compact and ordered carbon coating on solid-state behaviors of silicon during electrochemical processes. *Carbon Energy* **2020**, *2*, 143–150. [[CrossRef](#)]
13. Jung, D.S.; Hwang, T.H.; Park, S.B.; Choi, J.W. Spray Drying Method for Large-Scale and High-Performance Silicon Negative Electrodes in Li-Ion Batteries. *Nano Lett.* **2013**, *13*, 2092–2097. [[CrossRef](#)]
14. Feng, K.; Li, M.; Liu, W.; Kashkooli, A.G.; Xiao, X.; Cai, M.; Chen, Z. Silicon-Based Anodes for Lithium-Ion Batteries: From Fundamentals to Practical Applications. *Small* **2018**, *14*, 1702737. [[CrossRef](#)]
15. Chou, S.-L.; Pan, Y.; Wang, J.-Z.; Liu, H.-K.; Dou, S.-X. Small things make a big difference: Binder effects on the performance of Li and Na batteries. *Phys. Chem. Chem. Phys.* **2014**, *16*, 20347–20359. [[CrossRef](#)] [[PubMed](#)]
16. Liu, Z.; He, X.; Fang, C.; Camacho-Forero, L.E.; Zhao, Y.; Fu, Y.; Feng, J.; Kosteki, R.; Balbuena, P.B.; Zhang, J.; et al. Reversible Crosslinked Polymer Binder for Recyclable Lithium Sulfur Batteries with High Performance. *Adv. Funct. Mater.* **2020**, *30*, 2003605. [[CrossRef](#)]
17. Li, Z.; Fang, C.; Qian, C.; Zhou, S.; Song, X.; Ling, M.; Liang, C.; Liu, G. Polyisoprene Captured Sulfur Nanocomposite Materials for High-Areal-Capacity Lithium Sulfur Battery. *ACS Appl. Polym. Mater.* **2019**, *1*, 1965–1970. [[CrossRef](#)]
18. Zhu, T.; Liu, G. Communication—Functional Conductive Polymer Binder for Practical Si-Based Electrodes. *J. Electrochem. Soc.* **2021**, *168*, 050533. [[CrossRef](#)]
19. Chen, H.; Wu, Z.; Su, Z.; Chen, S.; Yan, C.; Al-Mamun, M.; Tang, Y.; Zhang, S. A mechanically robust self-healing binder for silicon anode in lithium ion batteries. *Nano Energy* **2021**, *81*, 105654. [[CrossRef](#)]
20. Yen, J.-P.; Chang, C.-C.; Lin, Y.-R.; Shen, S.-T.; Hong, J.-L. Effects of Styrene-Butadiene Rubber/Carboxymethylcellulose (SBR/CMC) and Polyvinylidene Difluoride (PVDF) Binders on Low Temperature Lithium Ion Batteries. *J. Electrochem. Soc.* **2013**, *160*, A1811–A1818. [[CrossRef](#)]
21. Buqa, H.; Holzapfel, M.; Krumeich, F.; Veit, C.; Novák, P. Study of styrene butadiene rubber and sodium methyl cellulose as binder for negative electrodes in lithium-ion batteries. *J. Power Sources* **2006**, *161*, 617–622. [[CrossRef](#)]
22. Lestriez, B.; Bahri, S.; Sandu, I.; Roué, L.; Guyomard, D. On the binding mechanism of CMC in Si negative electrodes for Li-ion batteries. *Electrochem. Commun.* **2007**, *9*, 2801–2806. [[CrossRef](#)]
23. Erk, C.; Brezesinski, T.; Sommer, H.; Schneider, R.; Janek, J. Toward Silicon Anodes for Next-Generation Lithium Ion Batteries: A Comparative Performance Study of Various Polymer Binders and Silicon Nanopowders. *ACS Appl. Mater. Interfaces* **2013**, *5*, 7299–7307. [[CrossRef](#)]
24. Hochgatterer, N.S.; Schweiger, M.R.; Koller, S.; Raimann, P.R.; Wöhrle, T.; Wurm, C.; Winter, M. Silicon/Graphite Composite Electrodes for High-Capacity Anodes: Influence of Binder Chemistry on Cycling Stability. *Electrochem. Solid-State Lett.* **2008**, *11*, A76. [[CrossRef](#)]
25. Liu, W.-R.; Yang, M.-H.; Wu, H.-C.; Chiao, S.M.; Wu, N.-L. Enhanced Cycle Life of Si Anode for Li-Ion Batteries by Using Modified Elastomeric Binder. *Electrochem. Solid-State Lett.* **2005**, *8*, A100. [[CrossRef](#)]
26. Li, J.; Lewis, R.B.; Dahn, J.R. Sodium Carboxymethyl Cellulose: A Potential Binder for Si Negative Electrodes for Li-Ion Batteries. *Electrochem. Solid-State Lett.* **2007**, *10*, A17. [[CrossRef](#)]
27. Dimov, N.; Noguchi, H.; Yoshio, M. A chemometric investigation of the effect of the process parameters on the performance of mixed Si/C electrodes. *J. Power Sources* **2006**, *156*, 567–573. [[CrossRef](#)]

28. Ding, N.; Xu, J.; Yao, Y.; Wegner, G.; Lieberwirth, I.; Chen, C. Improvement of cyclability of Si as anode for Li-ion batteries. *J. Power Sources* **2009**, *192*, 644–651. [[CrossRef](#)]
29. Bridel, J.S.; Azaïs, T.; Morcrette, M.; Tarascon, J.M.; Larcher, D. Key Parameters Governing the Reversibility of Si/Carbon/CMC Electrodes for Li-Ion Batteries. *Chem. Mater.* **2010**, *22*, 1229–1241. [[CrossRef](#)]
30. Zuo, P.; Yang, W.; Cheng, X.; Yin, G. Enhancement of the electrochemical performance of silicon/carbon composite material for lithium ion batteries. *Ionics* **2011**, *17*, 87–90. [[CrossRef](#)]
31. Kim, H.; Seo, M.; Park, M.-H.; Cho, J. A Critical Size of Silicon Nano-Anodes for Lithium Rechargeable Batteries. *Angew. Chem. Int. Ed.* **2010**, *49*, 2146–2149. [[CrossRef](#)]
32. Zheng, H.; Ridgway, P.; Song, X.; Xun, S.; Chong, J.; Liu, G.; Battaglia, V. Comparison of Cycling Performance of Lithium Ion Cell Anode Graphites. *ECS Trans.* **2011**, *33*, 91–100. [[CrossRef](#)]